Biol. Cell (2010) **102**, 479–488 (Printed in Great Britain) doi:10.1042/BC20100036

Research article

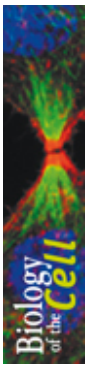

Munc18 and Munc13 regulate early neurite outgrowth

Jurjen H.P. Broeke*[1], Martijn Roelandse*†‡[1], Maartje J. Luteijn*, Tatiana Boiko*, Andrew Matus‡, Ruud F. Toonen* and Matthijs Verhage*[2]

*Department of Functional Genomics, Center for Neurogenomics and Cognitive Research, Neuroscience Campus Amsterdam, Vrije Universiteit (VU) and VU Medical Center (VUmc), De Boelelaan 1085, 1081 HV Amsterdam, The Netherlands, †Netherlands Institute for Neuroscience, Molecular Visual Plasticity, Meibergdreef 47, 1105 BA Amsterdam, The Netherlands, and ‡Department of Neurobiology, Friedrich Miescher Institute, Maulbeerstrasse 66, 4058 Basel, Switzerland

Background information. During development, growth cones of outgrowing neurons express proteins involved in vesicular secretion, such as SNARE (soluble *N*-ethylmaleimide-sensitive fusion protein-attachment protein receptor) proteins, Munc13 and Munc18. Vesicles are known to fuse in growth cones prior to synapse formation, which may contribute to outgrowth.

Results. We tested this possibility in dissociated cell cultures and organotypic slice cultures of two release-deficient mice (Munc18-1 null and Munc13-1/2 double null). Both types of release-deficient neurons have a decreased outgrowth speed and therefore have a smaller total neurite length during early development [DIV1–4 (day *in vitro* 1–4)]. In addition, more filopodia per growth cone were observed in Munc18-1 null, but not WT (wild-type) or Munc13-1/2 double null neurons. The smaller total neurite length during early development was no longer observed after synaptogenesis (DIV14–23).

Conclusion. These data suggest that the inability of vesicle fusion in the growth cone affects outgrowth during the initial phases when outgrowth speed is high, but not during/after synaptogenesis. Overall, the outgrowth speed is probably not rate-limiting during neuronal network formation, at least *in vitro*. In addition, Munc18, but not Munc13, regulates growth cone filopodia, potentially via its previously observed effect on filamentous actin.

Introduction

During early development, neurons form various indifferent processes, neurites, each bearing a growth cone at its tip (Goslin and Banker, 1989). In order to extend these neurites, the insertion of plasma membrane proteins and phospholipids is necessary (Goslin and Banker, 1989) to expand the plasma membrane. Phospholipids can reach the outgrowing neurite via either lateral diffusion of lipids incorporated at the soma or via lipid droplets and vesicles, thereby contributing to the necessary membrane expansion for outgrowth (Vance et al., 2000).

The vesicle release machinery that operates in mature neurons is already present in developing neurons at the tip of the growth cone (Igarashi et al., 1996; Kimura et al., 2003). This machinery is used for the release of synaptic vesicles containing neurotransmitter, which is thought to depend on SNARE (soluble *N*-ethylmaleimide-sensitive fusion protein-attachment protein receptor) proteins (Igarashi et al., 1996) and to be distributed along the whole axonal surface (Hua et al., 2005). These vesicles are thought to mature by repetitive recycling throughout axons (Krueger et al., 2003). From these vesicles, a plethora of molecules is released that have a role in neurite

[1]These authors have contributed equally to this work.
[2]To whom correspondence should be addressed (email matthijs.verhage@cncr.vu.nl).
Key words: development, growth cone, Munc18, neurite outgrowth, organotypic cultures, vesicle release.
Abbreviations used: AA, arachidonic acid; Arp2/3 complex, actin-related protein 2/3 complex; CDC42, cell division cycle 42; dGBSS, dissection Gey's balanced salt solution; DIV, day *in vitro*; E18, embryonic day 18; EGFP enhanced green fluorescent protein; HBSS, Hanks balanced salt solution; M13, Munc13-1 and Munc13-2; M18, Munc18-1; MAP2, microtubule-associated protein 2; NA, numerical aperture; PFA, paraformaldehyde; PLA, phospholipase A_2; SNARE, soluble *N*-ethylmaleimide-sensitive fusion protein-attachment protein receptor; WT, wild-type.

guidance and trophic support. In addition, vesicular fusion is considered to add lipids to the outgrowing neurites (Futerman and Banker, 1996).

Another source of lipids that may contribute to the outgrowing neurites are lipid droplets. These lipid droplets are trafficked in both directions along microtubules (Pol et al., 2004) and consist of lipids coated with a single phospholipid leaflet. The SNARE-dependent release machinery has previously been found to be associated with lipid droplets in fibroblasts (Bostrom et al., 2007).

As SNARE-dependent membrane fusion has been implicated in the supply of membrane and proteins to developing neurites, loss of this function is expected to result in abnormalities in long-distance projections and synaptogenesis. However, this does not seem to be true in two cases where expression of proteins essential for SNARE-dependent membrane fusion were genetically deleted: knockout mice of M18 (Munc18-1) (referred to as 'M18 null'; Verhage et al., 2000) and knockout mice of M13 (Munc13-1 and Munc13-2) (referred to as 'M13 null'; Varoqueaux et al., 2002). Both these mutants lack spontaneous and evoked vesicle release, but develop long-distance projections and contain many synapses at birth (Varoqueaux et al., 2002; Bouwman et al., 2004). In order to investigate this apparent discrepancy, we examined the effect of SNARE-dependent membrane fusion on initial neurite outgrowth in two reduced systems in a quantitative manner, namely primary and organotypic slice cultures during early development. Our data indicate that initial outgrowth *in vitro* is indeed impaired in fusion-defective mutant neurons when neurites grow out at maximal speed and that the morphology of growth cones is abnormal in the case of M18 null neurons. However, this impaired outgrowth apparently is not rate-limiting and does not prevent the eventual formation of normal neuronal networks in more mature primary and organotypic cultures, in line with previous observations *in vivo* (Varoqueaux et al., 2002; Bouwman et al., 2004).

Results

We set out to study the effect of SNARE-dependent synaptic vesicle release on early neurite development using low-density cultures of cortical or hippocampal neurons. We took advantage of two transgenic mouse lines that lack protein(s) involved in vesicle release, Munc18-1 (Verhage et al., 2000) and Munc13-1/2 (Varoqueaux et al., 2002). Genetic deletion of Munc18-1 (M18 null) or of Munc13-1 and Munc13-2 (M13 null) in mice completely abolishes spontaneous and evoked neurotransmitter release in neurons. Both mutations result in neonatal lethality. However, tissue derived from either of these lines can be cultured for a period of time (Varoqueaux et al., 2002; Heeroma et al., 2004).

We crossed these mice with mice bearing EGFP (enhanced green fluorescent protein) tagged to their membrane (EGFP-tKras; Roelandse et al., 2003) in order to visualize morphological alterations in fine neuronal structure. We focused on neurite extension and growth cone morphology during the first week in culture using dissociated cultures.

Outgrowth is decreased in release-deficient Munc18-1 null neurons from DIV3 (day 3 *in vitro*) onwards

As was shown previously in Munc13-1/2 null neurons, there is no vesicle cycle as measured by FM4-64-dye uptake (Varoqueaux et al., 2002). To test whether this also holds true for Munc18-1 null neurons, we examined FM4-64-dye uptake in WT (wild-type) and Munc18-1 null neurons. For these first experiments, neurons were grown on glass without an astrocyte feeder layer to reduce the background signal of FM4-64-dye taken up by astrocytes. Under these culture conditions, the morphology of growth cones is slightly different from growth cones in glia-supported or organotypic slice cultures (see below). We found that Munc18-1 null neurons indeed lacked FM4-64-dye uptake, indicating that there was no vesicle cycle (Figure 1, M18 null). Because the incorporation of lipids is a necessary component for the expansion of the membrane in outgrowing neurites, we examined whether the loss of lipids from synaptic vesicles decreased neurite outgrowth (for a review, see Vance et al., 2000). To this end, we used dissociated cortical neurons from DIV1 to DIV4 and measured total neurite length of WT and release-deficient Munc18-1 null neurons. Examples of traced neurons show that the initiation of neurite outgrowth occurred in all genotypes (Figure 2A). However, release-deficient neurons lagged behind in length as compared with WT neurons (Figures 2A and 2B, Munc18 and Munc13). This effect became apparent after 3 days in culture (19.6% reduction in length for Munc18-1 null neurons and

Figure 1 | Munc18-1 null neurons are deficient in vesicle recycling

In order to investigate the endocytosis of release-deficient Munc18-1 null neurons, an FM4-64 dye uptake experiment was done. After loading the cells using stimulation with 60 mM KCl and washing for 10 min with Tyrode's solution, WT neurons show punctuate staining in the growth cone (top row), which is not the case for the M18 null growth cone (bottom row). Scale bar, 5 μm.

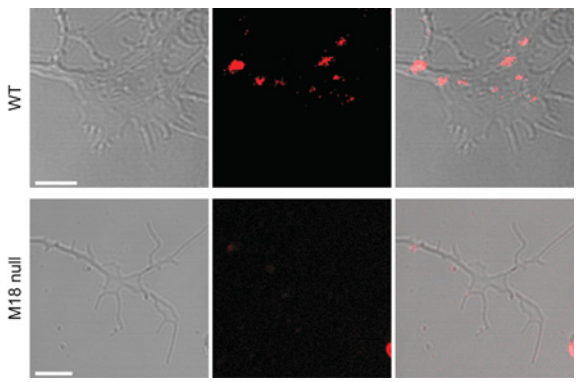

51.4% for Munc13-1/2 null neurons) and increased significantly on the fourth day (40.0% reduction in M18 and 61.1% in M13; Figure 2B). We therefore examined the speed of outgrowth at DIV3, as release-deficient neurons start to lag behind the WT neurons from this moment onwards.

Decreased outgrowth in release-deficient neurons is not caused by cell death

The early onset of cell death in dissociated cultures of Munc18-1 null, starting at approx. DIV4, may explain the decreased outgrowth. We therefore switched to organotypic hippocampal slice cultures where Munc18-1 null neuron survival exceeds DIV7. We cross-bred WT and Munc18-1 null mice with mice expressing EGFP tagged to their membrane (EGFP-tKras; Roelandse et al., 2003), in order to visualize morphological alterations in fine neuronal structure. In these organotypic cultures, neurons extend long neurites, most likely axons originating from the CA1 area of the hippocampus (Frotscher and Heimrich, 1993) that reach far into the surrounding matrix, which is permissive for neurite outgrowth, as shown previously (McKinney et al., 1999). We then measured the speed of outgrowth into the surrounding matrix, as the total neurite length could not be established in the densely packed network of outgrowing processes and somata in the slice itself. We also included Munc13-1/2 null animals (Figure 3A, M13 null) to further exclude cell death as a confounding effect in the changes in outgrowth speed. The outgrowth during the time-lapse series was reduced in the release-deficient cultures (Munc18-1 null and Munc13-1/2 null in Figure 3A; the red line indicates the starting point). Quantification showed a 42% and 46% ($P < 0.001$; t test M18: $n = 85$; M13: $n = 87$) decrease in outgrowth speed for Munc18-1 null and Munc13-1/2 null respectively compared with WT neurons ($n = 92$; Figure 3B). We also found a strong reduction in the accumulated distance (Figure 3C), showing a delayed outgrowth within our 20 min time frame.

Munc18-1 influences the number of filopodia

As the growth cone is important in neurite extension and guidance, we examined growth cone morphology in organotypic hippocampal slice cultures. In slices, the release-deficient cells survive longer. We therefore analysed morphology in slices and not in dissociated cultures. We visualized the dynamics of growth cone morphology in a projection of a 60-min time-lapse (Figure 4A). Munc13-1/2 null neurons showed a decreased growth cone palm area as compared with WT, whereas M18 null neurons appeared to have an increased growth cone area as compared with Munc13, but this was not significant (Figure 4B). Release-deficient M18 null growth cones did possess more filopodia per growth cone (Figure 4C). Overall, no differences were found in the filopodia length (Figure 4D). These data suggest that vesicle release is not important for growth cone morphology, but instead Munc13 influences growth cone area (Figure 4B), whereas Munc18 influences the number of filopodia (Figure 4C) but not their length (Figure 4D). Because filopodia contain mostly actin filaments, we investigated the influence of Munc18-1 on the actin cytoskeleton in dissociated cultures. By comparing the area of actin and dividing it by the area of tubulin in the growth cone (Figure 5A), we found that Munc18-1 null growth cones had an increase in actin content of 35% (Figure 5B).

Impaired vesicle release does not decrease long-term outgrowth

Although the release-deficient neurons show a decreased neurite outgrowth, the brain of release-deficient

Figure 2 | Developmental time course shows lagging of release-deficient neurites

(**A**) Neurite length was visualized by tracing the neurites at the indicated time points; showing decreased overall length and decreased arbour complexity in release-deficient M18 null and M13 null neurons. (**B**) Quantification of the neurite length showed that, during development, release-deficient neurons lagged behind in overall neurite length from DIV3 onwards. Means ± S.E.M. are plotted. DIV1 WT: $n = 285$; M18: $n = 211$; M13: $n = 404$; DIV2 WT: $n = 146$; M18: $n = 124$; M13: $n = 212$; DIV3 WT: $n = 135$; M18: $n = 62$; M13: $n = 169$; DIV4 WT: $n = 83$; M18: $n = 34$; M13: $n = 136$.

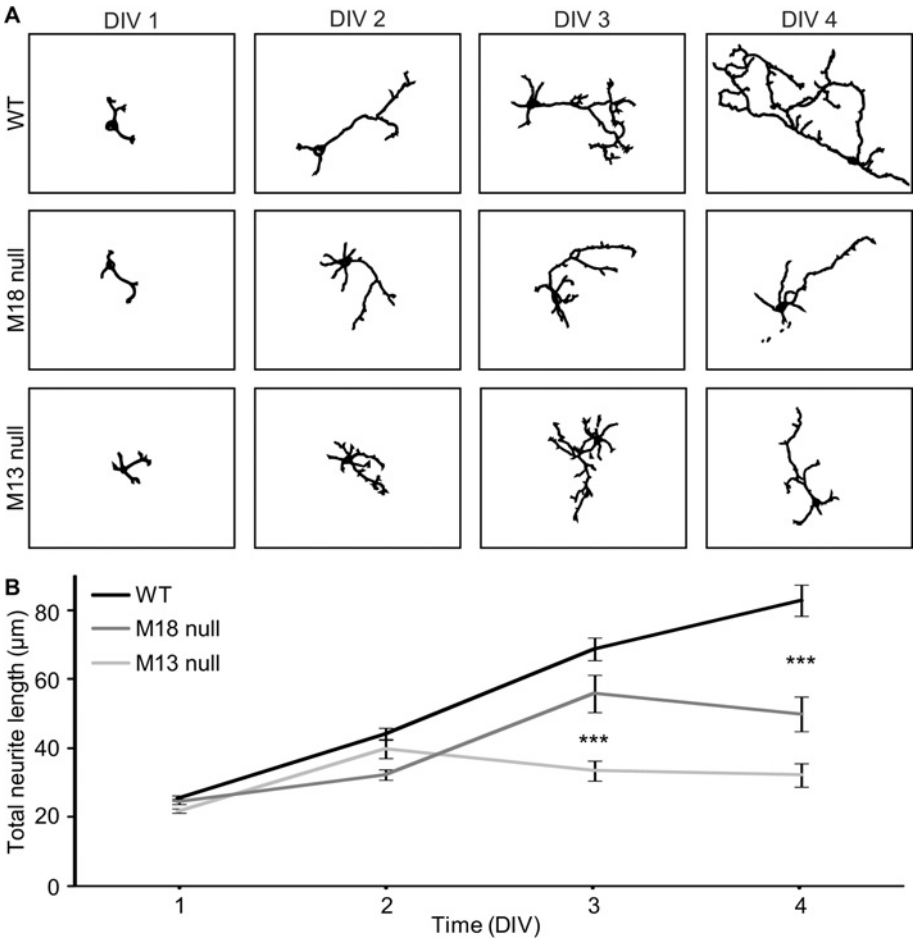

mice at embryonic day 18 developed normally (Verhage et al., 2000; Varoqueaux et al., 2002). We therefore examined the total dendrite length in older cultures of WT and M13 null hippocampal neurons. We chose for dendrite length, as the axon is difficult to trace and can extend several hundreds of micrometres within 1 week (Dotti et al., 1988). As Munc18-1 null neurons die before DIV7 (Heeroma et al., 2004), only WT and Munc13-1/2 null cultures were included. At DIV14, both WT and Munc13-1/2 null neurons were well established with numerous dendrites [MAP2 (microtubule-associated protein 2)-positive processes] per cell (Figure 6A). We measured the total dendrite length per field of view in both release-deficient Munc13-1/2 null cultures and WT cultures and found that the total dendrite length had not been affected in the release-deficient neurons when compared with WT neurons (Figure 6B). These data suggest that long-distance connections can be formed even with decreased outgrowth speed early in development. Synapse staining using a synapsin1 antibody revealed similar numbers of putative synapses (synapsin-positive deposits in close proximity to the dendritic arbour) in both WT and Munc13-1/2 null cultures (Figure 6A). This could still be observed at DIV23, where dendrite density is

Figure 3 | Vesicle release is involved in outgrowth speed

Quantification of outgrowth speed in slices at DIV3 shows differences between release-deficient and WT neurons. (**A**) Five frames taken from a 20-min time-lapse series at the indicated time points (top) showing the progression of a growth cone in an organotypic slice culture into the surrounding matrix. The red line indicates the starting position of the growth cone at $t = 0$ min. (**B**) Quantification of the speed of outgrowth showing a large decrease for M18 null (46 %) and M13 null (42 %) as compared with WT. (**C**) The average accumulated distance during the 20 min time-lapse was severely reduced in both release-deficient genotypes (blue and red curves) as compared with WT control (black curve). Scale bar in (**A**) is 3 μm. Means ± S.E.M. are plotted. ***$P < 0.001$; numbers in bars indicate the number of growth cones.

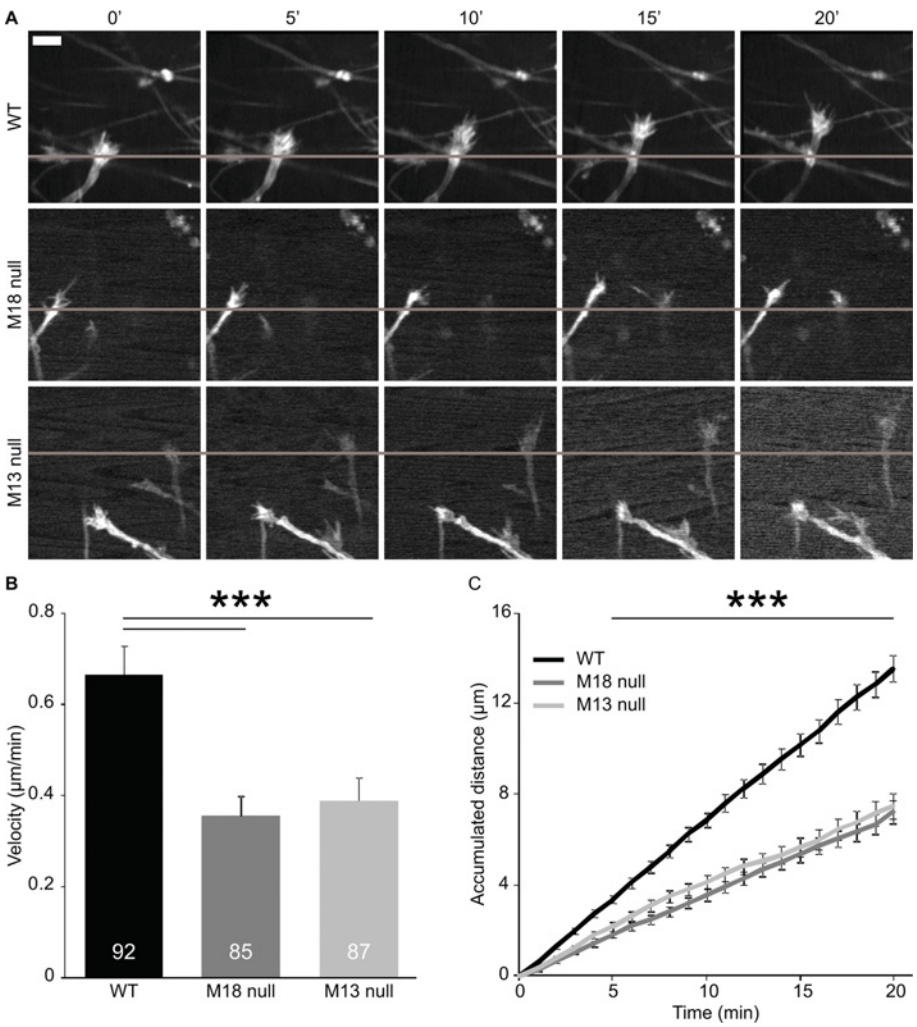

similar between WT and Munc13-1/2 null cultures (Figure 6C).

Discussion

During the first week of development, neurons extend their processes over long distances in order to form connections between brain areas. We found neurite length and rate of outgrowth in neurons that lack SNARE-dependent vesicle release to be diminished. This reduction became apparent approx. 3 days in culture and was significantly reduced at 4 days in culture, but did not abolish outgrowth entirely. Here, we have shown that the loss of two key proteins involved in synaptic vesicle recycling reduce neurite outgrowth in both hippocampus and cortex, which is most likely the result of a reduction in the

Figure 4 | Growth cone morphology is altered in M18-1 null neurons

Shown is an overlay of the first frame (red) and a projection of its consecutive frames (green) in a 60-min time-lapse. (**A**) Projected time-lapse series of the indicated genotypes showing distinct differences in morphology in M18 null growth cones. (**B**) Quantification of the growth cone palm area showed a decrease in M13 null. (**C**) Compared with WT, M18 null had an increased number of filopodia per growth cone, but this was not seen in M13 null. (**D**) The average length per filopodium showed no apparent differences. The scale bar in (**A**) is 2 μm. Means ± S.E.M. are plotted. $^*P < 0.05$; numbers in bars represent the number of growth cones (**B**, **C**) or the number of filopodia (**D**).

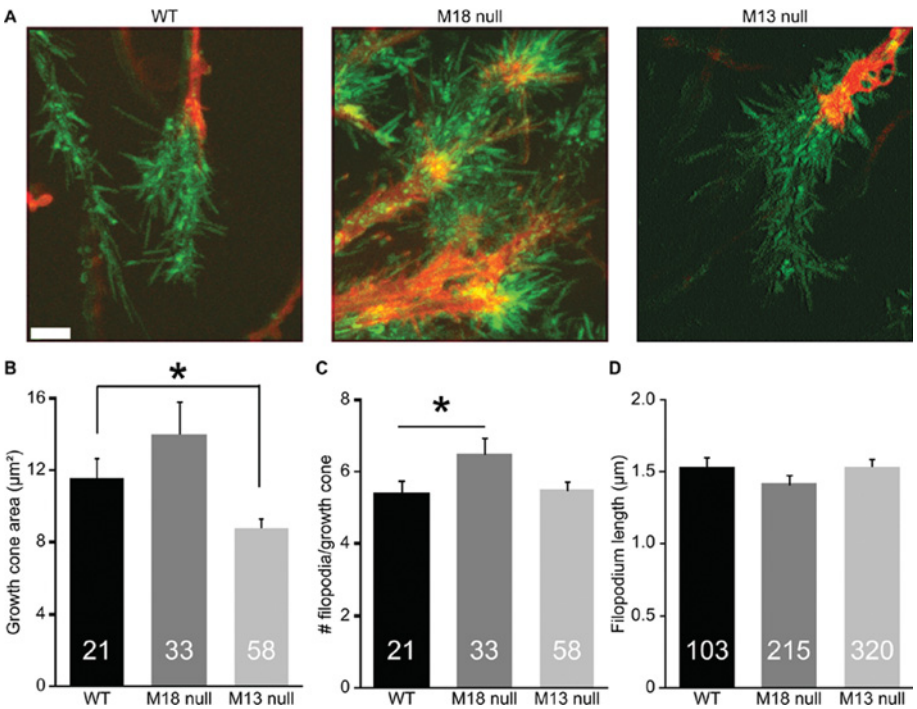

amount of lipids added to the membrane. This is in line with evidence from outgrowth in PC12 cells (Morihara et al., 1999) and hippocampal neurons (Grosse et al., 1999), where SNAP-25 (25 kDa synaptosome-associated protein) was cleaved by botulinum neurotoxin, causing a lack of vesicle exocytosis and resulted in reduced outgrowth.

Using synaptic vesicle parameters established by Takamori et al. (2006), we calculate that a spontaneous release rate of approx. One vesicle per second (Wyllie et al., 1994) and a neurite diameter of 440 nm (Takamori et al., 2006) can account for 0.12 μm of neurite extension per minute in lipids alone. The total surface area of a vesicle – lipids and proteins – accounts for 0.24 μm of neurite extension per minute, but vesicle proteins and some lipids are retrieved by endocytosis in outgrowing growth cones (Schenk et al., 2003). Importantly, the release-deficient neurons showed a decrease in outgrowth that was of the same order of magnitude, indicating that the loss of lipids supplied by vesicle fusion can in principle explain the reduction in outgrowth observed in the release-deficient neurons. Reduction in outgrowth for downstream SNARE proteins has been shown previously (Osen-Sand et al., 1993; Igarashi et al., 1996; Hirling et al., 2000). Furthermore, our observations show that this process occurs in different brain regions such as the cortex and hippocampus, independent of cell origin. However, the underlying mechanism for the reduced outgrowth remains to be elucidated.

Morphological changes in filopodia were observed in Munc18-1 null growth cones. This difference may be related to the manner in which Munc18-1 affects the actin cytoskeleton as shown here and in earlier

Figure 5 | Munc18-1 influences the actin cytoskeleton
Staining for actin (green) and tubulin (red) in WT and Munc18-1 null cultures was used to quantify the effect of Munc18 protein on the actin cytoskeleton (**A**). The area of actin and tubulin was measured and the ratio was taken. Compared with WT, Munc18-1 null growth cones had a 35 % increase in actin content (**B**). Bar in overview is 10 μm, zoomed picture is 5 μm. Means ± S.E.M. are plotted.

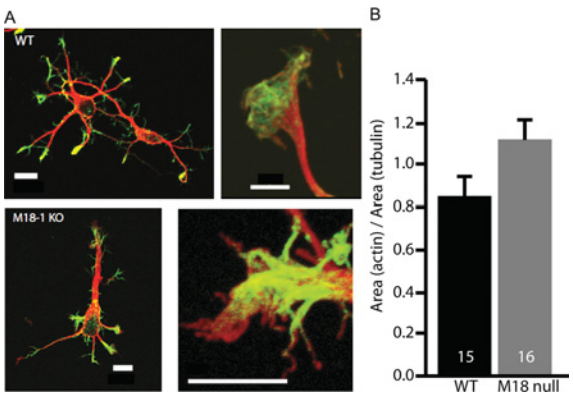

studies (de Wit et al., 2006; Toonen et al., 2006), influencing growth cone morphology via a mechanism that regulates the formation of filopodia. In this scheme, filopodium formation is dependent on the Arp2/3 complex (actin-related protein 2/3 complex), which forms a nucleation site for actin polymerization (for a review, see Mattila and Lappalainen, 2008), whereas filopodium extension is dependent on the Rho GTPase family, specifically CDC42 (cell division cycle 42; Nobes and Hall, 1995). Munc18-1 could regulate the binding of Arp2/3 complex to actin filaments, thereby manipulating the number of filopodia. Munc18-1 may also reduce CDC42 activity, thereby reducing filopodia extension. Finally, Munc18-1 null mutant mice have reduced cellular levels of syntaxin1 (Verhage et al., 2000; Bouwman et al., 2004), which may also contribute to the morphological changes observed in Munc18-1 null growth cones. However, we have shown before that syntaxin1 can still be readily detected in the terminal field of immature neurons *in vivo* (Toonen et al., 2005), suggesting that the availability of syntaxin is not a limiting factor. The morphological abnormalities observed in Munc18-1 null, but not Munc13-1/2 double null, growth cones may also relate to the previously observed effects of PLA (phospholipase A_2) and AA (arachidonic acid) in growth cones. The PLA/AA pathway appears to play a central role in growth cone morphology (de la Houssaye et al., 1999) and also modulates Munc18-1 function (Connell et al., 2007).

Lamellipodium formation influences the surface area of the cell (Nakaya et al., 2008) and is dependent on Rac1 (Nobes and Hall, 1995). Munc13 isoforms may decrease lamellipodia formation in the peripheral zone of the growth cone by influencing the Rho family GTPases (Kozma et al., 1997). This could result in an increased growth cone area in the Munc13-1/2 null neurons. However, our results were not conclusive about the effect of Munc13-1/2 on growth cone morphology.

Although release-deficient animals have a lethal phenotype, the reduced outgrowth speed is sufficient to form long-distance projections (Verhage et al., 2000; Varoqueaux et al., 2002). A rough calculation using outgrowth speeds found in cell culture showed that WT neurons have an outgrowth rate of ~1 mm/day, while release-deficient Munc18-1 and Munc13-1/2 null neurons have an outgrowth rate of ~0.6 mm/day. Neurite outgrowth starts at approx. E11–E12 (embryonic days 11–12) leaving 8–9 days until birth for outgrowth to proceed, allowing release-deficient neurons to attain a length of 5–10 mm which, given the dimensions of mouse neonatal brain, is sufficient to form long-distance connections. Consequently the loss of synaptic vesicle release in mutant neurons does not affect neurite outgrowth enough to prevent the formation of long-distance projections. A further factor in ameliorating the effects of decreased vesicle release could be that other mechanisms for incorporating lipids into growing membranes, coupled with lateral diffusion, are sufficient to supply the growing neurites with lipids. Such mechanisms, either singly or in combination, could account for our observations that, despite reductions in vesicle release, neurite length was capable of attaining WT levels in release-deficient neurons before the onset of, and during, synaptogenesis. Overall our data showed that molecular regulators of vesicular release, Munc18 and Munc13, contribute to neurite outgrowth. While mutant neurons can form long-distance synaptic connections, the delayed rate of outgrowth is significant at the early stages of neurite outgrowth and points to a potentially regulating role for Munc18 and Munc13 proteins in early neurogenesis, polarity and neurite extension.

Figure 6 | Decreased outgrowth recovers before synaptogenesis

All MAP2-positive neurites in a field of view were traced and the total dendrite length was divided by the number of somata. (**A**) Multiple fields of view were taken from WT (left) and M13 null (right) neurons at DIV14, showing a dense network of MAP2-positive neurites (green) originating from several somata (red asterisks). Furthermore, synapse staining (synapsin1, red) shows similar numbers of putative synapses in WT and Munc13-1/2 null neurons. (**B**) Quantification of dendrite length at DIV14, showing no significant difference (*t* test; WT: $n = 15$, M13: $n = 92$; $P = 0.48$) between WT and M13 null neurons. (**C**) Examples of neurons from WT and M13 null cultures at DIV23, showing comparable neurite length in kRas-EGFP labelled neurites. Scale bars: (**A**) 20 μm and (**C**) 100 μm. Means ± S.E.M. are plotted.

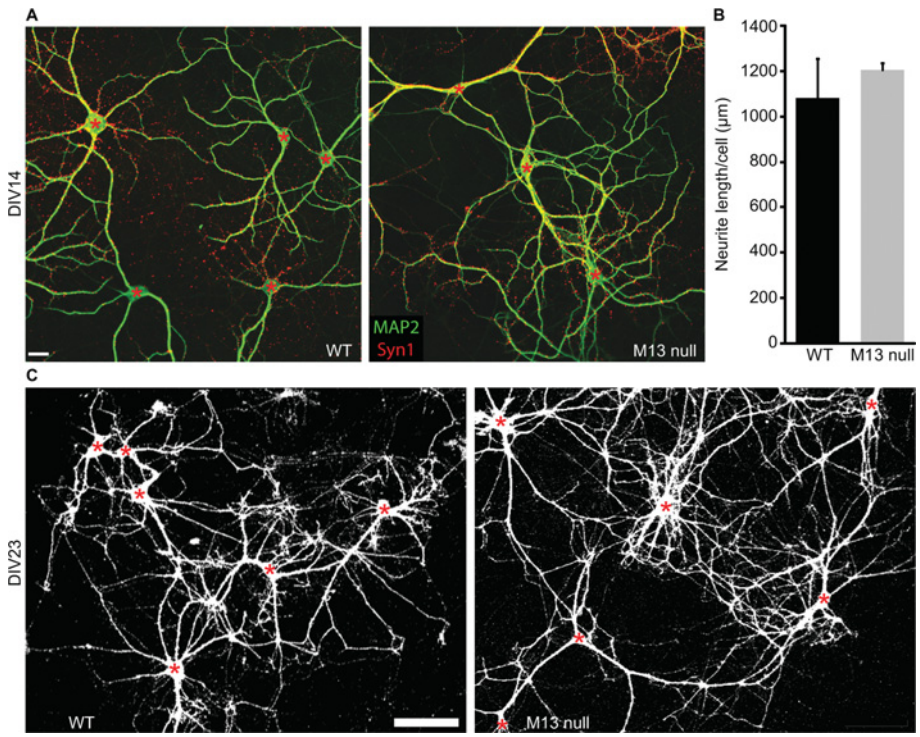

Materials and methods

Laboratory animals

Munc18-1 null, Munc13-1/2 double null and EGFP-tKras mice have been described previously (Verhage et al., 2000; Varoqueaux et al., 2002; Roelandse et al., 2003). Mouse embryos were obtained by caesarian section of pregnant females from timed heterozygous matings of EGFP-tKras with WT, with Munc18-1 heterozygous or with Munc13-1 heterozygous/Munc13-2 null animals (C57/Bl6 background). Animals were housed and bred according to Institutional, Dutch and U.S. governmental guidelines.

Dissociated cultures

Cortices or hippocampi were dissected from E18 mice and collected in HBSS (Hanks balanced salt solution; Sigma, St. Louis, MO, U.S.A.), buffered with 7 mM Hepes. After removal of the meninges, the cortices were minced and incubated for 20 min in trypsinized HBSS at 37°C. After washing the neurons were triturated with fire-polished Pasteur pipettes, counted with a haemocytometer and plated in Neurobasal medium (Invitrogen, Carlsbad, CA, U.S.A.) supplemented with 2% B-27 (Invitrogen), 1.8% Hepes, 1% GlutaMAX (Invitrogen), 1% Pen/Strep (Invitrogen) and 0.2% 2-mercaptoethanol (Sigma). Low-density cultures were plated on poly-L-lysine (Sigma)-coated glass coverslips at 25000 neurons/cm^2. For the analysis of early neurite outgrowth (DIV0–4), random images were taken of the cultures using a ×40 lens on a Leica MZ12 microscope. Cultures were fixed on DIV14 and DIV23 with 2% (w/v) PFA (paraformaldehyde; Invitrogen) and 2% sucrose for 20 min, and then 10 min in 4% PFA. After washing with PBS, the cultures were stained with a monoclonal anti-MAP2 antibody (Millipore, Billerica, MA, U.S.A.) in order to analyse neurite length. Synapses were stained with α-Synapsin1. Localization of Munc18-1 in growth cones was done by staining with α-Munc18-1 and α-Bassoon antibodies. Quantification of actin and tubulin was done by incubating cultures with phalloidin–Alexa Fluor® 488 and post-staining with an α-tubulin antibody.

Organotypic slice cultures

Organotypic slice cultures from E18 hippocampus were prepared as follows. Mouse embryos were obtained by caesarean section of

pregnant females from timed heterozygous mating. GFP (green fluorescent protein)-expressing animals were identified by direct inspection using a Leica MZ12 dissection microscope fitted with fluorescence optics. Hippocampi were dissected from brains in ice-cold dGBSS (dissection Gey's balanced salt solution; BioConcept, Allschwill, Switzerland) with 32 mM glucose and 1 mM kynurenic acid, pH 7.4) and cut into 400 μm thick slices using a McIlwain tissue chopper (Mickle Engineering, Gomshall, Guildford, Surrey, U.K.). These hippocampal slices were kept at 4°C in dGBSS for 60 min to recuperate. All subsequent procedures were identical with those described for organotypic slice cultures from P8 mice (Gähwiler, 1981). Briefly, Poly-D-lysine-coated coverslips were covered with chicken plasma, and a tissue slice was placed in the centre. An equal amount of thrombin was added to the plasma to form a plasma cloth. The organotypic slice cultures were left to recuperate for 1 h at room temperature (20°C) and then placed in a roller tube at 37°C.

Live cell imaging

For confocal imaging, slices were mounted on purpose-built chambers (Life Imaging Services, Olten, Switzerland) and observed in slice imaging medium containing 1 part HBSS with 7 mM Hepes and 1 part Liebovitz L15 medium with supplements (1.8% Hepes, 0.2% 2-mercaptoethanol, 2% B27 supplement and 1% GlutaMAX) using a Yokogawa microlens Nipkow confocal system (PerkinElmer, Life Science Resources, Cambridge, U.K.). Images were acquired using a cooled CCD (charge-coupled device) camera (Hamamatsu photonics) every minute for 20 min using a ×60 water lens [NA (numerical aperture) = 1.20]. Overview pictures were made using a ×40 oil objective (NA = 1.20) or a ×10 air objective (NA = 0.40) on a LSM510 microscope (Carl Zeiss, Jena, Germany).

FM4-64-dye uptake experiment

Dissociated cultures were cultured on glass coverslips coated with PDL (population doubling level) and imaged on DIV3 on a Zeiss confocal using a ×40 oil objective (NA = 1.20) at 37°C using perfusion of Tyrode's solution [containing (in mM): 115 NaCl; 2.5 KCl; 2 $CaCl_2$; 2 $MgSO_4$; 30 glucose]. FM4-64 (Invitrogen) was diluted in high-potassium Tyrode's solution (regular Tyrode's, but with 61.5 mM NaCl and 60 mM KCl) and added to the cells for 1 min. After washing for 10 min with Tyrode's solution, brightfield and fluorescence images were taken.

Data analysis

Analysis of neurite length was done by manually tracing the neurites using Metamorph software (Universal Imaging Corporation, West Chester, PA, U.S.A.). For the analysis of neurite outgrowth in DIV3 hippocampal slice cultures various parameters were analysed using MetaMorph software using the 'Track Points' function. Growth cone velocity and accumulated distance were calculated from this tracking of growth cones that extended into the surrounding matrix outside the slice. For the growth cone morphology, growth cones in the first frame of a 20 min time-lapse were analysed using ImageJ software (National Institutes of Health, Bethesda, MD, U.S.A.). The growth cone area was determined by drawing a polygon around the palm of the growth cone and filopodia length by drawing lines.

Visualization of growth cone morphology was done by flattening a 1 h time-lapse series and combining it with the first frame of the original time-lapse series. Before overlaying these pictures, the flattened time-lapse series was made green, while the first frame was made red. Statistical testing was done using SPSS software (SPSS, Chicago, IL, U.S.A.) and Excel, using Student's t test and a significance level of $P < 0.05$.

Author contribution

Matthijs Verhage, Andrew Matus, Ruud Toonen and Martijn Roelandse conceived the project and reviewed the manuscript. Jurjen Broeke and Matthijs Verhage wrote the manuscript. Jurjen Broeke and Martijn Roelandse collected data on organotypic slice cultures. Maartje Luteijn and Tatiana Boiko collected data on primary cultures.

Acknowledgements

We thank Nils Brose (Max Planck Institute for Experimental Medicine, Goettingen, Germany) for supplying mice and reviewing the manuscript. We also thank the technicians Joost Hoetjes and Desiree Schut for genotyping and culturing, as well as the animal caretakers Joke Wortel and Chris van der Meer for their excellent contributions.

Funding

This work was supported by the Geheugenprocessen en Dementie (GpD) [grant number 970-10-036 (to M.V.)]; a Zorgonderzoek Nederland en Medische Wetenschappen (ZonMW) Pionier Grant [grant number 900-01-001 (to M.V.)]; the Neuro-Bsik Mouse Phenomics Consortium [grant number BSIK03053]; and the EUSynapse Project [contract number 019055].

References

Bostrom, P., Andersson, L., Rutberg, M., Perman, J., Lidberg, U., Johansson, B.R., Fernandez-Rodriguez, J., Ericson, J., Nilsson, T., Boren, J. and Olofsson, S. (2007) Snare proteins mediate fusion between cytosolic lipid droplets and are implicated in insulin sensitivity. Nat. Cell Biol. **9**, 1286–1293

Bouwman, J., Maia, A.S., Camoletto, P.G., Posthuma, G., Roubos, E.W., Oorschot, V.M.J., Klumperman, J. and Verhage, M. (2004) Quantification of synapse formation and maintenance *in vivo* in the absence of synaptic release. Neuroscience **126**, 115–126

Connell, E., Darios, F., Broersen, K., Gatsby, N., Peak-Chew, S., Rickman, C. and Davletov, B. (2007) Mechanism of arachidonic acid action on syntaxin-munc18. EMBO Rep. **8**, 414–419

de la Houssaye, B.A., Mikule, K., Nikolic, D. and Pfenninger, K.H. (1999) Thrombin-induced growth cone collapse: involvement of phospholipase A_2 and eicosanoid generation. J. Neurosci. **19**, 10843–10855

de Wit, H., Cornelisse, L.N., Toonen, R.F.G. and Verhage, M. (2006) Docking of secretory vesicles is syntaxin dependent. PLoS One **1**, e126

Dotti, C.G., Sullivan, C.A. and Banker, G.A. (1988) The establishment of polarity by hippocampal neurons in culture. J. Neurosci. **8**, 1454–1468

Frotscher, M. and Heimrich, B. (1993) Formation of layer-specific fiber projections to the hippocampus *in vitro*. Proc. Natl. Acad. Sci. U.S.A. **90**, 10400–10403

Futerman, A.H. and Banker, G.A. (1996) The economics of neurite outgrowth – the addition of new membrane to growing axons. Trends Neurosci. **19**, 144–149

Goslin, K. and Banker, G. (1989) Experimental observations on the development of polarity by hippocampal neurons in culture. J. Cell Biol. **108**, 1507–1516

Grosse, G., Grosse, J., Tapp, R., Kuchinke, J., Gorsleben, M., Fetter, I., Höhne-Zell, B., Gratzl, M. and Bergmann, M. (1999) SNAP-25 requirement for dendritic growth of hippocampal neurons. J. Neurosci. Res. **56**, 539–546

Heeroma, J.H., Roelandse, M., Wierda, K., van Aerde, K.I., Toonen, R.F.G., Hensbroek, R.A., Brussaard, A., Matus, A. and Verhage, M. (2004) Trophic support delays but does not prevent cell-intrinsic degeneration of neurons deficient for munc18-1. Eur. J. Neurosci. **20**, 623–634

Hirling, H., Steiner, P., Chaperon, C., Marsault, R., Regazzi, R. and Catsicas, S. (2000) Syntaxin 13 is a developmentally regulated snare involved in neurite outgrowth and endosomal trafficking. Eur. J. Neurosci. **12**, 1913–1923

Hua, J.Y., Smear, M.C., Baier, H. and Smith, S.J. (2005) Regulation of axon growth *in vivo* by activity-based competition. Nature **434**, 1022–1026

Igarashi, M., Kozaki, S., Terakawa, S., Kawano, S., Ide, C. and Komiya, Y. (1996) Growth cone collapse and inhibition of neurite growth by botulinum neurotoxin c1: a t-SNARE is involved in axonal growth. J. Cell. Biol. **134**, 205–215

Kimura, K., Mizoguchi, A. and Ide, C. (2003) Regulation of growth cone extension by SNARE proteins. J. Histochem. Cytochem. **51**, 429–433

Kozma, R., Sarner, S., Ahmed, S. and Lim, L. (1997) Rho family GTPases and neuronal growth cone remodelling: relationship between increased complexity induced by Cdc42hs, Rac1, and acetylcholine and collapse induced by RhoA and lysophosphatidic acid. Mol. Cell. Biol. **17**, 1201–1211

Krueger, S.R., Kolar, A. and Fitzsimonds, R.M. (2003) The presynaptic release apparatus is functional in the absence of dendritic contact and highly mobile within isolated axons. Neuron **40**, 945–957

Mattila, P.K. and Lappalainen, P. (2008) Filopodia: molecular architecture and cellular functions. Nat. Rev. Mol. Cell Biol. **9**, 446–454

McKinney, R.A., Lüthi, A., Bandtlow, C.E., Gähwiler, B.H. and Thompson, S.M. (1999) Selective glutamate receptor antagonists can induce or prevent axonal sprouting in rat hippocampal slice cultures. Proc. Natl. Acad. Sci. U.S.A. **96**, 11631–11636

Morihara, T., Mizoguchi, A., Takahashi, M., Kozaki, S., Tsujihara, T., Kawano, S., Shirasu, M., Ohmukai, T., Kitada, M., Kimura, K. et al. (1999) Distribution of synaptosomal-associated protein 25 in nerve growth cones and reduction of neurite outgrowth by botulinum neurotoxin a without altering growth cone morphology in dorsal root ganglion neurons and PC-12 cells. Neuroscience **91**, 695–706

Nakaya, M., Kitano, M., Matsuda, M. and Nagata, S. (2008) Spatiotemporal activation of rac1 for engulfment of apoptotic cells. Proc. Natl. Acad. Sci. U.S.A. **105**, 9198–9203

Nobes, C.D. and Hall, A. (1995) Rho, Rac, and Cdc42 GTPases regulate the assembly of multimolecular focal complexes associated with actin stress fibers, lamellipodia, and filopodia. Cell **81**, 53–62

Osen-Sand, A., Catsicas, M., Staple, J.K., Jones, K.A., Ayala, G., Knowles, J., Grenningloh, G. and Catsicas, S. (1993) Inhibition of axonal growth by SNAP-25 antisense oligonucleotides *in vitro* and *in vivo*. Nature **364**, 445–448

Pol, A., Martin, S., Fernandez, M.A., Ferguson, C., Carozzi, A., Luetterforst, R., Enrich, C. and Parton, R.G. (2004) Dynamic and regulated association of caveolin with lipid bodies: modulation of lipid body motility and function by a dominant negative mutant. Mol. Biol. Cell **15**, 99–110

Roelandse, M., Welman, A., Wagner, U., Hagmann, J. and Matus, A. (2003) Focal motility determines the geometry of dendritic spines. Neuroscience **121**, 39–49

Schenk, U., Verderio, C., Benfenati, F. and Matteoli, M. (2003) Regulated delivery of AMPA receptor subunits to the presynaptic membrane. EMBO J. **22,**, 558–568

Takamori, S., Holt, M., Stenius, K., Lemke, E.A., Grønborg, M., Riedel, D., Urlaub, H., Schenck, S., Brügger, B., Ringler, P. et al. (2006) Molecular anatomy of a trafficking organelle. Cell **127**, 831–846

Toonen, R.F.G., de Vries, K.J., Zalm, R., Südhof, T.C. and Verhage, M. (2005) Munc18-1 stabilizes syntaxin 1, but is not essential for syntaxin 1 targeting and snare complex formation. J. Neurochem. **93**, 1393–1400

Toonen, R.F., Kochubey, O., de Wit, H., Gulyas-Kovacs, A., Konijnenburg, B., Sorensen, J.B., Klingauf, J. and Verhage, M. (2006) Dissecting docking and tethering of secretory vesicles at the target membrane. EMBO J. **25**, 3725–3737

Gähwiler, B.H. (1981) Organotypic monolayer cultures of nervous tissue. J. Neurosci. Meth. **4**, 329–342

Vance, J.E., Campenot, R.B. and Vance, D.E. (2000) The synthesis and transport of lipids for axonal growth and nerve regeneration. Mol. Cell. Biol. Lipids **1486**, 84–96

Varoqueaux, F., Sigler, A., Rhee, J., Brose, N., Enk, C., Reim, K. and Rosenmund, C. (2002) Total arrest of spontaneous and evoked synaptic transmission but normal synaptogenesis in the absence of munc13-mediated vesicle priming. Proc. Natl. Acad. Sci. U.S.A. **99**, 9037–9042

Verhage, M., Maia, A.S., Plomp, J.J., Brussaard, A.B., Heeroma, J.H., Vermeer, H., Toonen, R.F., Hammer, R.E., van den Berg, T.K., Missler, M. et al. (2000) Synaptic assembly of the brain in the absence of neurotransmitter secretion. Science **287**, 864–869

Wyllie, D.J.A., Manabe, T. and Nicoll, R.A. (1994) A rise in postsynaptic Ca^{2+} potentiates miniature excitatory postsynaptic currents and AMPA responses in hippocampal neurons. Neuron **12**, 127–138

Received 24 March 2010/7 May 2010; accepted 19 May 2010

Published as Immediate Publication 19 May 2010, doi:10.1042/BC20100036